

- A. Fischer and E. Sackman, *Nature* **313**, 299 (1985); A. Fischer, M. Lösche, H. Möhwald, E. Sackmann, *J. Phys. Lett.* **45**, L-785 (1984); A. Fischer and E. Sackmann, *J. Phys.* **45**, 517 (1984).
8. J. Dubochet, J. Lepault, R. Freeman, J. A. Berri-man, J.-C. Homo, *J. Microsc.* **128**, 219 (1982); J. Lepault, F. P. Booy, J. Dubochet, *ibid.* **129**, 89 (1983); M. Adrian, J. Dubochet, J. Lepault, A. W. McDowell, *Nature* **308**, 32 (1984); J. Dubochet *et al.*, *Rev. Biophys.* **21**, 129 (1988).
 9. J. L. Burns, Y. Cohen, Y. Talmon, *J. Phys. Chem.* **94**, 5308 (1990); A. Walter, P. K. Vinson, A. Kaplan, Y. Talmon, *Biophys. J.* **60**, 1315 (1991); R. G. Laughlin, R. L. Munyon, J. L. Burns, Y. Talmon, *J. Phys. Chem.* **96**, 474 (1992); N. Kamenka, M. Chorro, Y. Talmon, R. Zana, *Colloids Surf.* **67**, 213 (1992); R. Zana and Y. Talmon, *Nature* **362**, 228 (1993).
 10. Colloid-carbon-coated grids of 400 mesh, prepared according to a conventional technique [W. Baumeister and M. Hahn, in *Principles and Techniques of Electron Microscopy*, M. Hayat, Ed. (Van Nostrand Reinhold, New York, 1978), pp. 21–33 and 37–46], were placed on a stainless steel mesh in a specially prepared Teflon trough under the water subphase. Monolayers were spread (~70% available surface) on the surface of an aqueous solution at 20°C. The subphase was then cooled to 5°C, a temperature at which GIXD studies have shown the uncompressed monolayers to be highly crystalline. The water subphase was slowly drained with a motor-driven syringe, and the grids with the deposited monolayers were transferred to the plunging device [J. R. Bellare, H. T. Davis, I. F. Scriven, Y. Talmon, *J. Electron Microsc. Tech.* **10**, 87 (1988)]. Excess water on the underside of the grid was blotted with filter paper, and the grids were rapidly plunged into liquid ethane cooled

by liquid nitrogen to its freezing point. Such fast cooling has been found to vitrify the aqueous subphase, that is, to inhibit ice crystallization. The specimens were loaded into a Gatan 626 cold stage and examined in a Philips CM12 transmission electron microscope operated at 100 kV. The grids were maintained at -175°C throughout their examination, and dark-field technique was applied to obtain images of individual domains. To minimize radiation damage, low-dose precautions were used. However, even under low-dose conditions the specimens remained intact for 10 s or less.

11. Observed reflections from hexagonal ice, albeit rare, were used to calibrate the camera length and so permit the *d* spacings to be determined with sufficient accuracy.
12. F. Leveiller, D. Jacquemain, L. Leiserowitz, K. Kjaer, J. Als-Nielsen, *J. Phys. Chem.* **96**, 10380 (1992).
13. D. M. Small, in *Handbook of Lipid Research* (Plenum, New York, 1986), vol. 4, chaps. 2, 4, 5, and 8.
14. The maximum error in the determination of the unit cell dimensions is ~5%.
15. R. Popovitz-Biro *et al.*, unpublished data.
16. P. Curie, *J. Phys.* **3**, 393 (1894).
17. M. Gavish, R. Popovitz-Biro, M. Lahav, L. Leiserowitz, *Science* **250**, 973 (1990).
18. J. Majewski *et al.*, unpublished data.
19. E. E. Uzgiris and R. D. Kornberg, *Nature* **301**, 125 (1983).
20. We thank I. Weissbuch and R. Popovitz-Biro for discussions and J. Als-Nielsen and K. Kjaer for the cooperative venture into the GIXD experiments. Supported by the Minerva Foundation and the Petroleum Research Fund of the American Chemical Society.

16 March 1993; accepted 23 June 1993

Early and Late Alkali Igneous Pulses and a High-³He Plume Origin for the Deccan Flood Basalts

Asish R. Basu, Paul R. Renne, Deb K. DasGupta, Friedrich Teichmann, Robert J. Poreda

Several alkalic igneous complexes of nephelinite-carbonatite affinities occur in extensional zones around a region of high heat flow and positive gravity anomaly within the continental flood basalt (CFB) province of Deccan, India. Biotites from two of the complexes yield ⁴⁰Ar/³⁹Ar dates of 68.53 ± 0.16 and 68.57 ± 0.08 million years. Biotite from a third complex, which intrudes the flood basalts, yields an ⁴⁰Ar/³⁹Ar date of 64.96 ± 0.11 million years. The complexes thus represent early and late magmatism with respect to the main pulse of CFB volcanism 65 million years ago. Rocks from the older complexes show a ³He/⁴He ratio of 14.0 times the air ratio, an initial ⁸⁷Sr/⁸⁶Sr ratio of 0.70483, and other geochemical characteristics similar to ocean island basalts; the later alkalic pulse shows isotopic evidence of crustal contamination. The data document 3.5 million years of incubation of a primitive, high-³He mantle plume before the rapid eruption of the Deccan CFB.

A common model for the origin of CFB provinces is that they are generated by mantle plumes (1). In this model, partial melting initiated by the arrival of the hot plume thins and conductively heats the

lithosphere. Further rise of the plume through the lithosphere causes rapid eruption of the CFB (2, 3). The distinct geochemical and isotopic signatures of the CFB (4) support such a plume origin, although others have suggested (5) an upper mantle or lithospheric source for CFB. In this report, we provide age and geochemical evidence from three of the alkalic igneous complexes of the Deccan trap CFB of peninsular India that document the chemical evolution of this rising plume through the

continental lithosphere over a 3.5-million-year time interval.

The western Indian crustal plate can be divided into a number of segments separated by fracture zones radiating from the Cambay basin (Fig. 1), an area of high heat flow associated with well-defined positive gravity anomalies (6, 7). A number of alkali-carbonatite bodies associated with the Deccan tholeiites crop out along the Narmada Valley, a rift extending eastward from the Cambay basin (Fig. 1), and along another prominent fault zone parallel to the western coast of India, extending through the Cambay basin possibly as much as 600 km to the north (8). This fault zone also contains alkalic rocks of the Bombay area (9). The Girnar (10) and the Phenai Mata (11) alkali complexes, all volcanic plugs, follow essentially an east-west trend (Fig. 1). A connection between the Maldiveridge, an oceanic north-south lineament off the west coast, and the Deccan Traps in the mainland is indicated by seismic refraction profiles of the western Indian Ocean (12). The Sarnu-Dandali and Mundwara alkalic complexes (Fig. 1) are situated approximately at the northward extension of the Maldiveridge through the West Coast fault, Panvel Flexure, and the Cambay Graben. Drilling in the gravity high near Kadi in the Cambay basin has recovered nepheline syenite at the base of the Tertiary sediments (13). The alkali rocks of Sarnu and Mundwara (14) and Kadi may be aligned along a zone extending to the southern end of the Cambay basin; the alkalic plugs and flows of central Kutch (Fig. 1) may also belong to a zone connecting this basin. These correlations indicate that the Deccan province extends beyond the present-day boundaries of the traps (Fig. 1), particularly to the north.

The Mundwara magmatic complex (Fig. 1) occurs as ring-shaped and plug-like intrusions within the Erinpura granite of Proterozoic age in Rajasthan (24°50'N, 72°33'E). Two units of the complex, Toa and Mer, show arcuate, ring-shaped hills (2 to 3 km in diameter), whereas the third, Musala, is a single conical hill about 1 km in diameter (15, 16). Ultramafic and mafic rocks are dominant in the Toa complex; the Mer intrusion is composed mostly of alkaline mafic rocks. Mafic rocks also dominate the Musala plug, but some felsic rocks, such as foid syenites and foid monzosyenites, are also present. All three intrusions have chilled margins and contain many dikes of diabase, basalts, microsyenites, phonolites, and lamprophyres. In addition, carbonatite dikes intrude rocks outside the Mer ring. The distribution of alkaline mafic rocks and syenites in association with more mafic and ultramafic differentiates, such as picrites and pyroxenites, implies that all these rock

A. R. Basu, F. Teichmann, R. J. Poreda, Department of Geological Sciences, University of Rochester, Rochester, NY 14627.

P. R. Renne, Institute of Human Origins, Geochronology Center, Berkeley, CA 94709.

D. K. DasGupta, Department of Geology, Presidency College, Calcutta, India 700073.

types may have formed from parental alkali olivine basalt magma, which occurs as flows in Toa (16, 17). The intrusive history of the entire Mundwara complex fits the established sequence of fractionation of alkali olivine basalt magma from alkalic ultramafic through alkalic mafic to alkalic syenites. The Sarnu-Dandali complex, located approximately 150 km northwest of Mundwara (Fig. 1), comprises a variety of acid, intermediate, and alkalic rocks, including plugs of ijolites, foidal syenites, and dikes of carbonatites.

We dated primary biotite from an alkali olivine gabbro (Mundwara #79) of the Toa pluton by incremental laser-heating $^{40}\text{Ar}/^{39}\text{Ar}$ analysis of two separate grains (18). The two grains yielded indistinguishable apparent age plateaus (Fig. 2A) with ages of 68.50 ± 0.22 (14 steps) and 68.57 ± 0.24 million years ago (Ma) (13 steps). The weighted mean of the two plateau dates is 68.53 ± 0.16 Ma (2σ). We also analyzed separately two individual grains of hornblende (Mundwara #51) from a brown-amphibole-bearing melagabbro in the Mundwara complex by incremental laser heating, both of which yielded saddle-shaped apparent age spectra with minimum step ages at ~ 71 Ma. Neglecting (air-rich) lower temperature steps from each grain revealed a linear array of 16 points of data on an isotope correlation diagram (Fig. 3) that is reasonably interpreted as a mixture between (i) inherited Ar with $^{40}\text{Ar}/^{36}\text{Ar} = 473 \pm 5$ and (ii) radiogenic Ar corresponding to an age of 69.36 ± 1.26 Ma (2σ), indistinguishable from the biotite results.

Three separate analyses of grains of bi-

otite from an alkali pyroxenite (Sarnu #C-11) of the Sarnu-Dandali complex (Fig. 1) gave well-defined apparent age plateaus (Fig. 2B) of 68.63 ± 0.16 (19 steps), 68.59 ± 0.22 (15 steps), and 68.53 ± 0.12 Ma (16 steps), with a weighted mean of 68.57 ± 0.08 Ma.

The geochronologic data from Mundwara and Sarnu-Dandali clearly indicate that alkali magmatism began 3.5 million years before the main pulse of Deccan volcanism at 65 Ma (2, 19). The spatial-temporal relation between these complexes and the Deccan flood basalts centered 600 km to the south is consistent with northward motion of the Indian plate at 10 to 15 cm/year over a nascent Reunion hotspot. This observation may indicate that the Cambay Graben was active 3.5 million years before the rapid eruption of the bulk of the Deccan traps; it also documents the temporal and structural contiguities between the Mundwara and Sarnu-Dandali complexes and the Deccan traps.

Ten samples of different lithologies from the three Mundwara plutons show a conspicuous enrichment of light rare earth elements (REEs) relative to that in chondrites (Fig. 4A). The gabbro in Fig. 4A showing the lowest concentration has textural evidence of crystal settling and thus cannot represent the original parent liquid. The REE patterns imply that the Mundwara suite evolved from an initial liquid of basaltic composition by olivine and pyroxene fractionation. We modeled (Fig. 4B) the parent liquid composition by different degrees of batch melting of a parent mantle peridotite (20). The assumed starting perid-

otite composition is in the garnet peridotite mineral facies and thus may reflect a greater depth of derivation of the partial melt. These data collectively indicate that the mantle beneath India began to melt as early as 68.5 Ma at a greater depth to form the Mundwara alkalic parent magma; later, by 65 Ma, the mantle had melted extensively by a much larger degree of partial melting at a shallower level, perhaps in the stability field of spinel peridotites, to generate the voluminous tholeiites (21). This pattern of volcanism is consistent with models for the

Fig. 1. Sketch map of part of the Indian peninsula showing the approximate locations of alkalic igneous complexes of western and northwestern India that are associated with the Deccan Traps volcanism and its major structural-tectonic framework. Includes the Narmada-Son Lineament, Cambay Graben, Panvel Flexure (f), West Coast fault (a), and several other lineaments recognized from Landsat imageries (b, Koyna Lineament; c, Koyna Rift; d, Kurduvadi Rift; e, Ghat Lineament). Current exposures of Deccan traps are shown in stipples. Areas of positive gravity anomalies are shown in hatched patterns. Alkali complexes marked with stars: 1, Sarnu-Dandali, Barmer District, Rajasthan (36); 2, Mundwara, Sirohi District, Rajasthan (15, 36); 3, Mount Girnar, Gujarat (10); 4, Phenai Mata, Gujarat (34, 37); 5, Amba Dongar, Gujarat (11); 6, Netrang, Gujarat (8); 7, Kadi, Gujarat (13); 8, Barwaha, Madhya Pradesh (8); 9, Jawhar Nepheline Syenite Dike, near Bombay, and associated alkalic rocks of Bassein and Trombay (34, 37); and 10, alkali olivine basalt lava flows and plugs of central Kutch (38). [Modified from (7, 35)].

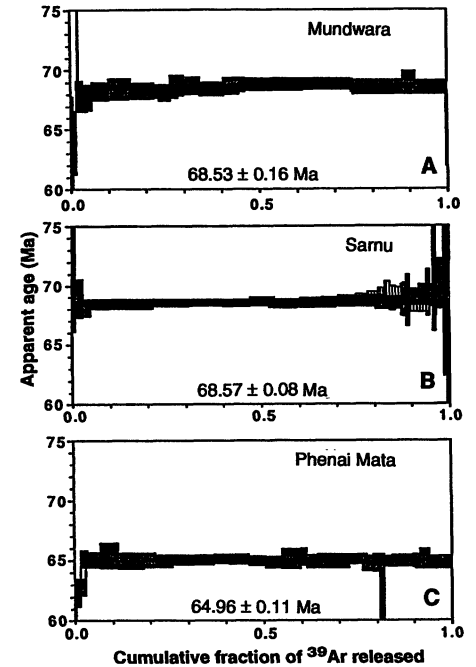
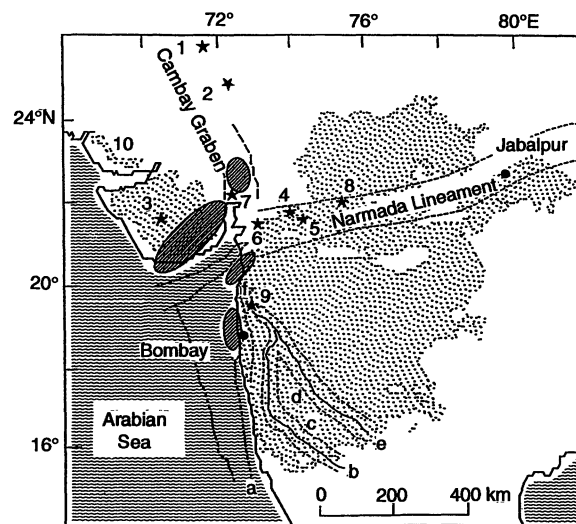


Fig. 2. Laser-heating $^{40}\text{Ar}/^{39}\text{Ar}$ apparent age spectra for biotites from the (A) Mundwara (two runs) (B) Sarnu-Dandali (three runs), and (C) Phenai Mata (two runs) complexes. Individual grains are distinguished by different ruling patterns; overlap is in black. The ages shown are inverse variance weighted means of the two plateaus, within 2σ intralaboratory errors that include contributions from error in the neutron fluence parameter J . Vertical width of boxes indicates 1σ errors calculated without error in J .

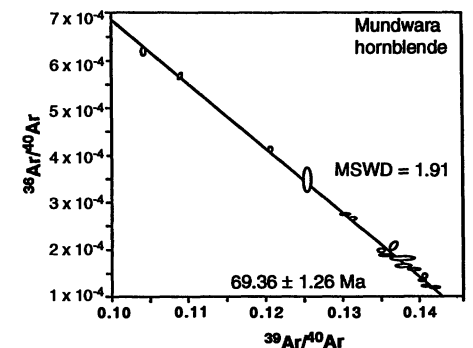


Fig. 3. Isotope correlation diagram for Mundwara hornblende showing 1σ error ellipses and regression line.

ascent of plumes through the continental lithosphere.

Phenai Mata is part of the Chota Udaipur carbonatite-alkalic district (Fig. 1), which covers 1200 km². In this area (22°7'N, 73°50'E) Precambrian metamorphic rocks are overlain by the Bagh (Late Cretaceous) sedimentary rocks; the latter are overlain by the Deccan traps. The northern part of this alkalic district includes a dike complex consisting mostly of phonolite, tinguaitite, and minor sovite. To the west stands Phenai Mata hill, a composite plug of gabbros, basalt, granophyre, nepheline syenite, trachyte, and tinguaitite. The undersaturated alkalic rocks of the Phenai Mata plug intruded into earlier formed Deccan trap flows of tholeiitic composition (22). Most of the rocks of the Phenai Mata suite show normative olivine and nepheline, and the degree of undersaturation is also reflected in the presence of minerals like nepheline, aegirine, and barkevikite.

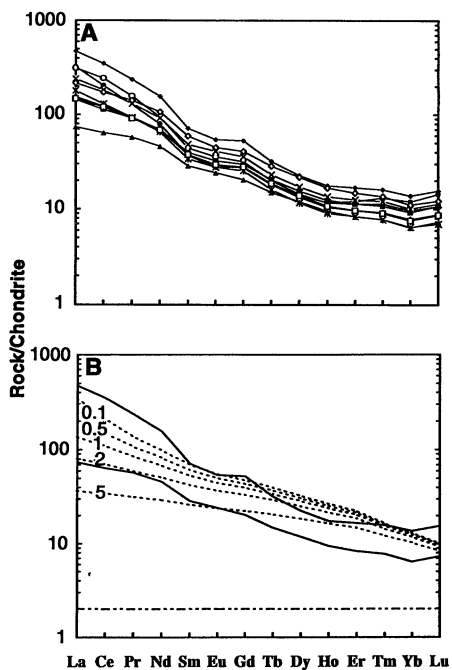


Fig. 4. (A) Inductively coupled plasma-mass spectrometric analyses of the concentration of REEs, normalized to chondritic abundances, in the various lithologic members of the Mundwara complex. Lithologic members: basalt (Δ), microsyenite (\bullet), syenite (\circ), theralite (\times), basalt (\times), gabbro (\blacksquare), picrite (\square), nepheline syenite (\blacklozenge), basalt (\diamond), and gabbro (\blacktriangle). (B) The observed patterns in the REE concentration of the Mundwara rocks (range outlined by two solid, continuous lines) can be matched (20) by 0.5 to 2% partial melting (dotted lines) of a garnet peridotite source with 70% olivine, 20% orthopyroxene, 7% clinopyroxene, and 3% garnet. In this modeling of the batch melting process, we assumed that the parent peridotite initially had twice the chondritic concentrations (dotted dashed line at bottom).

An olivine gabbro (#3-21) was selected for ⁴⁰Ar/³⁹Ar dating. This gabbro was part of a body that is intrusive into the main mass of trachybasalt, and it is a holocrystalline, coarse- to medium-grained rock; this body, in turn, is traversed by syenite and diabase dikes. Xenoliths of the flood basalts occur in the gabbro. Rhythmic and cryptic layering can be observed in the main exposure of this rock. Various geological aspects of the gabbro indicate a shallow level of emplacement and a relatively rapid rate of cooling. Analysis (18) of two separate bitotite grains of the gabbro yielded indistinguishable apparent age plateaus (Fig. 2C) of 64.99 ± 0.16 (15 steps) and 64.94 ± 0.14 Ma (15 steps); the weighted mean of these two is 64.96 ± 0.11 Ma (2σ). This age can be taken as the age of intrusion of the Phenai Mata alkalic complex, and it is identical, within error, to the age of the bulk of the Deccan traps at 65 Ma (2, 19). As the Phenai Mata complex intrudes the Deccan traps, this alkalic igneous intrusion was probably emplaced near the end of the Deccan volcanism on the Indian peninsula. The two different ages established above for the alkalic complexes are consistent with

results from petrological modeling of mantle solidus curves, thermal structure of mantle plumes, and magma generation (23) that predict eruption of nepheline normative and carbonatitic compositions in the early and late stages of formation of tholeiitic volcanic provinces by plume volcanism.

To characterize further the mantle source of the alkalic intrusions and by inference the source of the tholeiitic flood basalts, we examined the Rb-Sr systematics of the whole-rock samples and the isotopic composition and abundance of noble gases of olivine and pyroxene in alkalic mafic rocks from the Mundwara, Sarnu, and Phenai Mata complexes. We crushed the minerals under high vacuum to release the gases from inclusions in the minerals [see (24) for experimental and analytical details] and to minimize the contribution from radiogenic ⁴He or cosmogenic ³He, or both, contained in the crystal lattice of the mineral separates (25). Observed ³He/⁴He ratios are 13.9 and 10.5 times the air ratio (R_A) for the pyroxene separates from two different rocks of the Mundwara complex (Table 1). Pyroxenes from an alkali pyroxenite (C-11, Table 1) of the Sarnu complex

Table 1. Helium isotopic ratios and helium and neon abundances in the minerals of the alkalic complexes (age in parentheses) measured in stepwise crushing experiments. Helium isotope ratios are corrected for procedural blanks ($2 \pm 1 R_A$; He and Ne abundances of 0.2 and 0.40 ncc/g, respectively) and air contribution, assuming all neon is of atmospheric origin; this correction is <1.2% for first-stage crushes. Ol, olivine; Cpx, clinopyroxene; Alk, alkali.

Rock type	Sample no.	Minerals	Crush		³ He/ ⁴ He (R_A)	⁴ He (ncc/g)	²⁰ Ne (ncc/g)	(He/Ne)/(He/Ne) _{air}
			Stage	Duration (min)				
<i>Mundwara (68.5 Ma)</i>								
Ol pyroxenite	80	Cpx*	1	5	10.5 ± 0.3	100.5	3.64	87
			2	10	9.2 ± 0.3	88.0	2.40	116
			3	15	8.5 ± 0.3	43.2	4.25	32
Ol melagabbro	211	Cpx†	1	5	13.9 ± 0.3	73.0	2.00	115
			2	10	13.0 ± 2.0	7.7	0.80	30
<i>Sarnu (68.5 Ma)</i>								
Alk pyroxenite	C-11	Cpx‡	1	5	12.8 ± 0.2	290	3.5	260
			2	10	12.4 ± 0.2	510	3.1	520
<i>Phenai Mata (65.0 Ma)</i>								
Alk Ol gabbro	3-21	Ol	1	5	3.4 ± 0.1	590	0.60	3100
			Cpx	1	10	3.1 ± 0.1	285	0.20

*Titansalite. †Salite. ‡Aegirine-augite.

Table 2. The Rb-Sr systematics data of whole-rock samples in Table 1, normalized to ⁸⁶Sr/⁸⁸Sr = 0.1194. The NBS987 Sr standard analyzed in our laboratory gave ⁸⁷Sr/⁸⁶Sr = 0.710245(26). Number in parentheses is error in last two digits showing 2σ of the mean. Procedural blank yielded 50 pg of Rb and 200 pg of Sr.

Sample no.	Rb (ppm)	Sr (ppm)	⁸⁷ Rb/ ⁸⁶ Sr	⁸⁷ Sr/ ⁸⁶ Sr	
				Measured	Initial
80	4.1	328.9	0.0359	0.704999(30)	0.704964(30)
211	14.3	271.1	0.1518	0.704973(20)	0.704826(20)
C-11	58.7	551.7	0.3065	0.704788(20)	0.704492(20)
3-21	4.5	442	0.0293	0.706877(20)	0.706849(20)

also gave a high $^3\text{He}/^4\text{He}$ ratio of $12.8 R_A$. These ratios are higher than the average ratio ($8 R_A$) observed in mid-ocean ridge basalts (MORBs) and are consistent with results from many ocean island basalts. Such high $^3\text{He}/^4\text{He}$ ratios are commonly interpreted as diagnostic of a mantle plume that is sampling primordial or deep mantle. The high ratios at Mundwara and Sarnu represent a lower $^3\text{He}/^4\text{He}$ limit because preferential diffusion of ^3He from the crystal and radiogenic ^4He production by U and Th decay would reduce the initial $^3\text{He}/^4\text{He}$ ratio in 68.5 million years. The $^3\text{He}/^4\text{He}$ ratios in the Phenai Mata olivines and pyroxenes are lower at 3.4 to $3.1 R_A$ (Table 1), respectively, and are indicative of crustal contamination during this late pulse of plume volcanism.

Ratios of $^3\text{He}/^4\text{He}$ higher than those of MORBs are a common feature of many basalts at hotspots such as Reunion ($14 R_A$) (26), the present-day trace of the presumed plume that generated the Deccan flood basalts. A similar association between present-day mantle plumes and continental basalts has been made on the basis of elevated $^3\text{He}/^4\text{He}$ ratios for the basalts from the Ethiopia Rift and the Snake River plain in the western United States (27). The plume association for Mundwara and Sarnu is strengthened by $^{87}\text{Sr}/^{86}\text{Sr}$ data (Table 2). On a plot of $^3\text{He}/^4\text{He}$ versus $^{87}\text{Sr}/^{86}\text{Sr}$ (Fig. 5), the alkali rocks from Sarnu ($12.8 R_A$, 0.70449), Mundwara ($13.9 R_A$, 0.70483), and Phenai Mata (3.1 to $3.4 R_A$, 0.70685) fall on a mixing trajectory between a high- ^3He mantle plume component and a purely crustal He-Sr component ($<0.1 R_A$;

≈ 0.72). Mundwara and Sarnu complexes display initial $^{87}\text{Sr}/^{86}\text{Sr}$ ratios similar to those of the least contaminated Deccan tholeiitic lavas, such as those of the Ambenali formation in the upper sequence (7, 28). In addition to the mantle-derived Sr, the carbonatites of Mundwara, as well as those of the Sarnu-Dandali complex, have mantle carbon ($\delta^{13}\text{C}$) and oxygen ($\delta^{18}\text{O}$) values of -6.4 per mil (Pee Dee belemnite standard) and $+6.1$ per mil (standard mean ocean water), respectively (29). Neodymium-isotopic measurements (initial $\epsilon_{\text{Nd}} = -15$ to -5) of the Phenai Mata rocks are well within the field for crustal rocks (30), consistent with their He and Sr isotopic signatures.

The high $^3\text{He}/^4\text{He}$ ratio of 13.9 ± 0.3 times the atmospheric ratio in the pyroxenes of the 68.5-million-year-old alkalic complex demonstrates that He-isotopes can be used as tracers for detecting ancient mantle plumes and links the plumes to the generation of major CFB provinces. The association of the alkalic complexes within and in near proximity to the lineaments and grabens of western India signifies the structural controls and the mode of interaction between the Deccan mantle plume and the Indian continental plate. Regarding the controversy in flood basalt petrogenesis (31), the correlated He and Sr isotopic data, as presented above, favor a plume source from the lower mantle (4, 32) over a subcontinental lithospheric source (5, 33).

REFERENCES AND NOTES

1. M. A. Richards, R. A. Duncan, V. E. Courtillot, *Science* **246**, 103 (1989); I. H. Campbell and R. W. Griffiths, *Earth Planet. Sci. Lett.* **99**, 79 (1990).
2. R. A. Duncan and D. G. Pyle, *Nature* **333**, 841 (1988); V. Courtillot et al., *ibid.*, p. 843.
3. P. R. Renne and A. R. Basu, *Science* **253**, 176 (1991); P. R. Renne et al., *ibid.* **258**, 975 (1992).
4. M. Sharma, A. R. Basu, G. V. Nesterenko, *Geochim. Cosmochim. Acta* **55**, 1183 (1991); *Earth Planet. Sci. Lett.* **113**, 365 (1992).
5. C. J. Allegre, B. Dupre, P. Richard, D. Rousseau, *Earth Planet. Sci. Lett.* **57**, 25 (1982); R. W. Carlson, G. W. Lugmair, J. D. Maccougall, *Geochim. Cosmochim. Acta* **45**, 2483 (1981).
6. J. A. Glennie, *R. Astron. Soc. Geophys. J.* **6** (suppl.), 179 (1951); V. S. Krishnaswamy, *Geol. Soc. India Mem.* **3**, 1 (1981).
7. J. J. Mahoney, in *Continental Flood Basalts*, J. D. Maccougall, Ed. (Kluwer, Dordrecht, Netherlands, 1988), pp. 151-194.
8. D. D. Yellur, *J. Geol. Soc. India* **9**, 118 (1968); S. Subba Rao, *Bull. Volcanol.* **35**, 998 (1972); D. K. DasGupta, *Indian Geol. Assoc. Biannu. Bull.* **7**, 137 (1974); M. K. Bose, *J. Geol. Soc. India* **21**, 317 (1980).
9. Such as those of the Jawahar and Bassein area, north of Bombay; see (34).
10. K. K. Mathur, V. S. Dubey, N. L. Sharma, *J. Geol.* **34**, 289 (1926).
11. R. N. Sukeshwala and G. R. Udas, *Int. Geol. Congr.* **7**, 1 (1964); A. P. Subramaniam and M. L. Parimoo, in *Advancing Frontiers in Geology and Geophysics* (Indian Geophysical Union, Hyderabad, India, 1964), vol. 441; S. G. Viladkar, *Bull. Geol. Soc. Finl.* **53**, 17 (1981); A. G. Jhingran, *Rec. Geol. Surv. India* **83**, 501 (1954); K. V. Subba Rao, *Int. Geol. Congr.* **7**, 42 (1964); M. K. Bose,

- Contrib. Mineral. Petrol.* **39**, 247 (1973).
12. T. J. Francis and G. G. Shor, *J. Geophys. Res.* **71**, 427 (1966).
13. L. L. Bhandari, *Mineral Wealth* **4**, 1 (1968); S. Ramamathan, *Geol. Soc. India Mem.* **3**, 198 (1981).
14. T. H. D. La Touche, *Mem. Geol. Surv. India* **35** (no. 1), 75 (1902).
15. D. K. DasGupta, *Q. J. Geol. Min. Metall. Soc. India* **47**, 117 (1975).
16. M. K. Bose and D. K. Das Gupta, *Geol. Mag.* **110**, 457 (1973).
17. T. R. Sharma, *Indian Geosci. Assoc. J.* **11**, 79 (1969); M. K. Chakraborti and M. K. Bose, *J. Geol. Soc. India* **19**, 454 (1978).
18. $^{40}\text{Ar}/^{39}\text{Ar}$ dating was as described in (3). Samples were individual grains of biotite ~ 0.5 mm in diameter, hand picked and cleaned ultrasonically in distilled water. Fish Canyon sanidine (27.84 Ma) was used as a neutron fluence monitor. The (Mundwara and Phenai Mata) samples were coirradiated with the same nine Haitian tektites that yielded a weighted mean plateau age of 65.01 ± 0.08 Ma [C. C. Swisher et al., *Science* **257**, 954 (1992)]. Plateau steps for each biotite and high-temperature data for the Mundwara hornblende were also cast on $^{36}\text{Ar}/^{40}\text{Ar}$ versus $^{39}\text{Ar}/^{40}\text{Ar}$ isotope correlation diagrams. For the Mundwara biotite ($N = 27$), the isochron age was 68.58 ± 0.62 Ma, initial $^{40}\text{Ar}/^{36}\text{Ar}$ was 293.4 ± 10.3 , and mean squared weighted deviates (MSWD) was 1.33. For the Sarnu biotite ($N = 50$), the isochron age was 68.61 ± 0.52 Ma, initial $^{40}\text{Ar}/^{36}\text{Ar}$ was 295.5 ± 1.4 , and MSWD was 2.93. For the Phenai Mata biotite ($N = 30$), the isochron age was 64.94 ± 0.58 Ma, initial $^{40}\text{Ar}/^{36}\text{Ar}$ was 298.2 ± 4.3 , and MSWD was 0.96. Isochron regression used the method of D. York [*Earth Planet. Sci. Lett.* **5**, 320 (1969)].
19. A. K. Bakshi and E. Farrar, *Geology* **19**, 461 (1991).
20. In this modeling, we used distribution coefficients of the REE [D. McKenzie and R. K. O'Nions, *J. Petrol.* **32**, 1021 (1991)] and assumed that the parent rock initially had twice the concentration of chondrites. It is clear from Fig. 4B that the degree of partial melting was small, $<2\%$. About 1 to 0.5% partial melting is necessary to generate the REE pattern of the parent liquid of the Mundwara suite of igneous rocks.
21. A. R. Basu, M. Sharma, G. V. Nesterenko, *Eos* **73**, 43 (1992).
22. R. N. Sukeshwala and S. F. Sethna, *Neues Jahrb. Mineral. Abh.* **118**, 159 (1973); *J. Geol. Soc. India* **10**, 177 (1969).
23. P. J. Wyllie, *J. Geophys. Res.* **93**, 4171 (1988).
24. R. J. Poreda and K. Farley, *Earth Planet. Sci. Lett.* **113**, 129 (1992).
25. Successive crushing steps were used to evaluate the importance of any cosmogenic or radiogenic contribution to the He. As crushing proceeds, the amount of magmatic He in inclusion will decrease and any cosmogenic or radiogenic component will become more dominant. The fact that both pyroxene samples showed a decrease in $^3\text{He}/^4\text{He}$ in the later steps (Table 1) indicates that the release of radiogenic ^4He dominates over any potential cosmogenic ^3He contribution.
26. H. Craig and W. Rison, *Eos* **63**, 1144 (1982); D. Graham, J. Lupton, F. Albarede, M. Condomines, *Nature* **347**, 545 (1990). The sources of data in Fig. 5, other than Reunion: M. D. Kurz, W. J. Jenkins, S. R. Hart, D. Clague, *Earth Planet. Sci. Lett.* **66**, 388 (1983); A. Zindler and S. R. Hart, *Annu. Rev. Earth Planet. Sci.* **14**, 493 (1986); K. A. Farley, J. Natland, H. Craig, *Earth Planet. Sci. Lett.* **111**, 183 (1992); M. D. Kurz, W. J. Jenkins, S. R. Hart, *Nature* **297**, 43 (1982); M. D. Kurz, P. Meyer, H. Sigurdsson, *Earth Planet. Sci. Lett.* **74**, 291 (1985); R. J. Poreda, J. G. Schilling, H. Craig, *ibid.* **78**, 1 (1986).
27. H. Craig and P. Scarsi, *Eos* **73**, 542 (1992).
28. Z. X. Peng et al., in preparation.
29. N. P. Subrahmanyam and C. Leelanandam, *Geol. Soc. India Mem.* **15**, 25 (1989); A. Sarkar and S. K. Bhattacharya, *Curr. Sci.* **62**, 368 (1992).
30. A. Prinzhofer, C. J. Allegre, L. G. Gwalani, A. Nicholas, *Eos* **69**, 521 (1988).
31. D. J. DePaolo, *Geochim. Cosmochim. Acta* **47**,

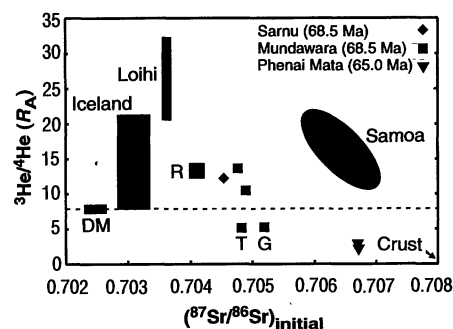


Fig. 5. $^3\text{He}/^4\text{He}$ (R_A) versus initial $^{87}\text{Sr}/^{86}\text{Sr}$ ratios in the pyroxene and olivine mineral separates of the alkalic complexes of Sarnu, Mundwara, and Phenai Mata, associated with the Deccan traps. The high He-isotope ratios reported in this study reflect primordial He in the plume source for the Deccan. This plume-source is clearly a high- ^3He source, not a low- ^3He (lower than a depleted MORB mantle), (DM) source as characterized by Tristan (T) and Gough (G) islands volcanic rocks. Fields of Loihi (Hawaii), DM (depleted MORB mantle), R (Reunion), Samoa, and Iceland are from (26), and that of the local continental crust is estimated.

841 (1983); R. W. Carlson, G. W. Lugmair, J. D. Maccougall, *ibid.*, p. 845.
 32. D. J. DePaolo and G. J. Wasserburg, *Proc. Natl. Acad. Sci. U.S.A.* **76**, 205 (1979); G. J. Wasserburg and D. J. DePaolo, *ibid.*, p. 3594.
 33. C. J. Hawkesworth *et al.*, *Geol. Soc. S. Afr. Spec. Publ.* **13**, 341 (1984); C. J. Hawkesworth, M. S. M. Mantovani, P. N. Taylor, Z. Palacz, *Nature* **322**, 356 (1986).
 34. R. N. Sukeshwala and R. K. Avasia, *J. Geol. Soc. India*, **7**, 86 (1966).
 35. K. B. Powar, *Geol. Soc. India Mem.* **3**, 45 (1981).
 36. A. L. Coulson, *Mem. Geol. Surv. India* **63**, 83 (1933); R. K. Srivastava, *Geol. Soc. India Mem.* **15**, 3 (1989).
 37. R. N. Sukeshwala and S. F. Sethna, *J. Geol. Soc. India* **10**, 177 (1969).

38. P. Krishnamurthy, K. Pande, K. Gopalan, J. D. Maccougall, *Geol. Soc. India Mem.* **10**, 53 (1988).
 39. Partially supported by National Science Foundation grants (EAR 9118008, EAR 9205054, EAR 9209719, and EAR 9206502) and the Institute of Human Origins. We are grateful to R. K. Srivastava for providing the Sarnu samples and to the staff and scientists of the Directorate of Geology and Mining, Gujarat State, for their assistance in the field-sampling and for sharing the geological information for many of the alkaline complexes mentioned in this study. Constructive comments by two anonymous reviewers improved the manuscript substantially.

8 March 1993; accepted 8 June 1993

Influence of Productivity on the Stability of Real and Model Ecosystems

John C. Moore,* Peter C. de Ruiter, H. William Hunt

The lengths of food chains within ecosystems have been thought to be limited either by the productivity of the ecosystem or by the resilience of that ecosystem after perturbation. Models based on ecological energetics that follow the form of Lotka-Volterra equations and equations that include material (detritus) recycling show that productivity and resilience are inextricably interrelated. The models were initialized with data from 5- to 10-year studies of actual soil food webs. Estimates indicate that most ecological production worldwide is from ecosystems that are themselves sufficiently productive to recover from minor perturbations.

Primary productivity and dynamic stability (the return to steady state after perturbation) have been treated as independent constraints on the length of food chains in ecosystems (1, 2). Systems differing greatly in productivity have food chains of similar length, and models indicate that longer food chains are less stable. Models often consist of primary producers, herbivores, and predators and exclude detritus, even though a high percentage of primary production is not consumed alive (3). When studies included energetics and detritus feedbacks, ecosystem productivity was found to influence food web diversity (4), structure (5), and resilience (6). In this report we develop models with and without detritus that include energetics as represented by birth and death rates, feeding rates, and assimilation and production efficiencies. We demonstrate that primary productivity affects the dynamic stability of food chains and, hence, their length. Few ecosystems worldwide are less productive (7) than the lower limits of productivity established by the models.

J. C. Moore, Department of Biological Sciences, University of Northern Colorado, Greeley, CO 80539.
 P. C. de Ruiter, Department of Soil Biology, DLO-Institute for Soil Fertility Research, 9750 RA Haren (Groningen), Netherlands.
 H. W. Hunt, Department of Range Science and the Natural Resource Ecology Laboratory, Colorado State University, Fort Collins, CO 80526.

*To whom correspondence should be addressed.

Food chains based on primary producers are frequently modeled after Lotka-Volterra:

$$\frac{dX_i}{dt} = r_i X_i - \sum_{j=1}^n c_{ij} X_i X_j \quad (1)$$

where X_i and X_j represent the population densities of primary producers and herbivores, respectively; r_i is the specific growth rate (birth minus death unrelated to herbivory); and c_{ij} are the coefficients of consumption of the primary producers by the herbivores. This equation does not adequately model detritus. Detritus can be modeled following DeAngelis *et al.* (6) where X_d represents the density of detritus

$$\begin{aligned} \frac{dX_d}{dt} = & R_d + \sum_{i=1}^n \sum_{j=1}^n (1 - a_j) c_{ij} X_i X_j \\ & + \sum_{i=1}^n d_i X_i - \sum_{j=1}^n c_{dj} X_d X_j \quad (2) \end{aligned}$$

Here R_d is input from an allochthonous source, for example, detritus inputs into streams. Additionally, detritus cycles autochthonously as the unassimilated fractions of prey killed, $\sum (1 - a_j) c_{ij} X_i X_j$, and the corpses of organisms that die from causes other than predation, $\sum d_i X_i$. The coefficient of consumption of the detritus by detritivores is represented by c_{dj} . Detritus is con-

sumed in a density-dependent manner similar to the way organisms are consumed (8, 9).

The growth equations for consumers, X_j , can be similar for primary producer and detritus models

$$\frac{dX_j}{dt} = -d_j X_j + \sum_{i=1}^n a_{ji} c_{ij} X_i X_j - \sum_{i=1}^n c_{ji} X_j X_i \quad (3)$$

Consumers die at a specific rate d_j and grow as a function of the prey consumed, $\sum c_{ij} X_i X_j$. The assimilation efficiency is a_j , and the production efficiency is p_j .

We define stability as unique to the region where all populations are at equilibrium X^* (10). If populations deviate by a small amount from their equilibria and then return, the chain is locally stable (10). Stability is assessed by evaluating the eigenvalues of the community matrix A whose elements α_{ij} are the partial derivatives of the equations for each species with respect to all species in the chain near equilibrium. Typically, α_{ij} are assigned values that ensure positive equilibrium densities and therefore only apply to a subset of matrix space where the chains are feasible. This approach has frustrated experimentation, as no direct field measures of the α_{ij} are practical (11). Here, α_{ij} were expressed as functions of measurable parameters: birth and death rates, energetic efficiencies, and consumption rates. Parameter values (d_j , c_j , a_j , and p_j) were sampled from the uniform distribution (0, 1). Values for nondimensional energy conversion efficiencies (a_i and p_i) are within these ranges by definition, and whether the range (0, 1) is plausible for the rate constants (d_i and c_{ij}) depends on the time and mass units chosen. The input rate for detritus R_d and the specific growth rate for primary producers r_i were set at increments of an order of magnitude beginning at 10^{-2} unit and ending with 10^5 units, encompassing a greater range of productivity than has yet been observed.

If the randomly selected parameters produced positive equilibrium densities for all species, the system was deemed feasible (12). For feasible systems, the parameter values and equilibrium densities were used to construct the elements of the community matrix A . Because all food chains in the analysis satisfied the criteria for qualitative stability (10), all feasible food chains were necessarily locally stable. The return time (RT) of a feasible system is the time required by the system to return to equilibrium after a perturbation and was estimated as $RT = -1/\text{real}(\lambda_{\max})$ (12), where $\text{real}(\lambda_{\max})$ is the real part of the largest eigenvalue. This process was repeated 1000 times for each productivity.

Productivity affected the feasibility of